2007-01-2489

Optimization-based Dynamic Human Walking Prediction

Y. Xiang, H.J. Chung, A. Mathai, S. Rahmatalla, J. Kim,
T. Marler, S. Beck, J. Yang, J.S. Arora, K. Abdel-Malek
Virtual Soldier Research Program, Center for Computer Aided Design, The University of Iowa, Iowa City, IA 52242, USA

John Obusek
U.S. Army Soldier Center, Natick, MA 01760, USA

ABSTRACT

In this study, an optimization-based approach for simulating the walking motion of a digital human model is presented. A spatial skeletal model having 55 degrees of freedom is used to demonstrate the approach. Design variables are the joint angle profiles. Walking motion is generated by minimizing the mechanical energy subjected to basic physical and kinematical constraints. A formulation for symmetric and periodic normal walking is developed and results are presented. Backpack and ground reaction forces are taken into account in the current formulation, and the effects of the backpack on normal walking are discussed.

INTRODUCTION

Simulation of 3D human walking is a challenging problem from analytical and computational points of view. An accurate biomechanical walking model is needed for product prototype design in industry. Several attempts have been made in the literature to develop realistic mechanical models. One approach uses motion capture data to perform simulations, or created libraries that can be used to query for a particular motion. Motion capture is an experiment-based approach where the motion of a subject is recorded by identifying the marker positions in the Cartesian coordinates. The joint angle trajectories are then generated by using the recorded data and the inverse kinematics. This approach is limited by the accuracy of the experimental data, and the simulated motion is subject-specific (McGuan, 2001).

A second approach is the ZMP-based trajectory generation method, which enforces stability of the mechanism during walking. With the preplanned zero moment point (ZMP) and feet location, the walking motion can be generated to follow the desired ZMP trajectory using an optimal control strategy (Yamaguchi et al., 1999; Kajita et al., 2003). The ZMP concept can also be incorporated in an optimization formulation to synthesize a walking pattern by maximizing the stability subject to physical constraints (Huang et al., 2001; Mu and Wu, 2003; Kim et al., 2005). The inverted pendulum model is another method that has been used to solve the walking problem because biped walking can be treated as an inverted pendulum. Advantages of this method are its simplicity and fast solvable dynamics equations (Park and Kim, 1998). However, it also suffers from an inadequate dynamics model that cannot generate natural and realistic human motion.

In addition to the previously mentioned methods, optimization-based trajectory generation is aimed at more realistic and natural humanoid motion. A model with large degrees of freedom (DOF) is not a problem, and many human-featured criteria can be considered simultaneously. For digital human simulations, the objective functions represent human performance measures, and optimization methods are used to solve for the feasible joint motion profiles that optimize an objective function and satisfy the necessary constraints (Chung et al., 2007; Thelen et al., 2003). Chevallereau and Aousin (2001) planned a robotic walking and running motion using optimization to determine the coefficients of a polynomial approximation for profiles of the pelvis translations and joint angle rotations. Walking was treated as a combination of successive single support phases with instantaneous double support phases defined by passive impact. Saidouni and Bessonnet (2003) solved for cyclic, symmetric gait motion of a nine-DOF model that moves in the sagittal plane. The control points for the B-spline curves along with the time durations for the gait stages are optimized to minimize the actuating torque energy. By adopting the time durations as design variables, the motion for the single support and the motion for the double support are simultaneously optimized. Anderson and Pandy (2001) developed a musculoskeletal model with 23 DOF and 54 muscles for normal symmetric walking on level ground using dynamic optimization method. Muscle forces were treated as design variables, and metabolic energy expenditure per unit distance was minimized. The forward dynamics was solved for kinematics, and ground reaction forces were obtained from the equilibrium condition in each iteration. The repeatable initial and final postures were given from the experimental data.

In the present work, an optimization-based predictive formulation based on the physics of motion (the dynamics of the motion) is developed; it relies on a few experimental data or not at all. Instead an objective function and appropriate constraints are defined to simulate natural human walking motion. This is called the predictive dynamics approach. The digital human model consists of 55 DOF, where a DOF characterizes a jointed pair of links in the kinematics sense, where various links of the body are assumed to be connected by revolute joints. Six DOF represent global translation and rotation and the other 49 represent the kinematics of the body. The resultant action of all the muscles at a joint is represented by the torque for each degree of freedom. The torques and angles at a joint are treated as unknowns in the optimization problem. The cubic B-spline interpolation is used for time discretization, and the well-established robotic formulation of the Denavit-Hartenberg method is used for kinematic analysis of the mechanical system. The recursive Lagrangian formulation is used to develop the equations of motion and was chosen because of its known computational efficiency. The approach is also suitable for evaluation of the gradients in closed form that are needed in the optimization process. The problem is formulated as a nonlinear optimization problem. A unique feature of the formulation, perhaps the most significant of this method, is that the equations of motion are not integrated explicitly. They are imposed simply as equality constraints in the optimization process, thus enforcing the laws of physics. A program based on a sequential quadratic programming approach is used to solve the nonlinear optimization problem. The control points for the joint angle profiles are treated as design variables. For the performance measure, the mechanical energy that is represented as the integral of the sum of the squares of all the joint torques is minimized. The dynamic stability is achieved by satisfying the ZMP constraint throughout the walking motion. The solution is simulated in the Santos™ environment and the results are validated and verified by examining two of the six standard determinants from experiments that characterize normal walking. In addition to the normal walking case, other cases that simulate walking with a shoulder backpack of varying loads are also addressed and the results are demonstrated.

SPATIAL HUMAN SKELETAL MODEL

The kinematics of the spatial human skeletal model of the current work is based on the Denavit-Hartenberg method.

DENAVIT-HARTENBERG METHOD

The kinematics relation of a spatial human model is represented by the Denavit-Hartenberg (DH) method, in which 4×4 homogeneous transformation matrices relate two adjacent coordinate systems (Denavit and Hartenberg, 1955). The DH transformation matrix includes rotation and translation and is a function of four parameters: θ_i, d_i, α_i, and a_i, as shown in Equation (1).

$$ {}^{i-1}\mathbf{T}_i = \begin{bmatrix} \cos\theta_i & -\cos\alpha_i \sin\theta_i & \sin\alpha_i \sin\theta_i & a_i \cos\theta_i \\ \sin\theta_i & \cos\alpha_i \cos\theta_i & -\sin\alpha_i \cos\theta_i & a_i \sin\theta_i \\ 0 & \sin\alpha_i & \cos\alpha_i & d_i \\ 0 & 0 & 0 & 1 \end{bmatrix} \quad (1) $$

In order to obtain a systematic representation of a serial kinematics chain, $\mathbf{q} \in R^n$ is defined as the vector of n-generalized coordinates, the joint angles. The position vector of a point of interest in the Cartesian space can be written in terms of the joint variables as $\mathbf{X} = \mathbf{X}(\mathbf{q})$. In this form, the augmented 4×1 vectors ${}^0\mathbf{r}_n$ and $\mathbf{r}_n$ are defined using the global Cartesian vector $\mathbf{X}(\mathbf{q})$ and the local Cartesian vector $\mathbf{X}_n$ as:

$$ {}^0\mathbf{r}_n = \begin{bmatrix} \mathbf{X}(\mathbf{q}) \\ 1 \end{bmatrix}; \quad \mathbf{r}_n = \begin{bmatrix} \mathbf{X}_n \\ 1 \end{bmatrix} \quad (2) $$

where $\mathbf{X}_n$ is the position of a point with respect to the n^{th} coordinate system. Using these vectors, ${}^0\mathbf{r}_n$ can be related to $\mathbf{r}_n$ as follows:

$$ {}^0\mathbf{r}_n = {}^0\mathbf{T}_n(\mathbf{q})\ \mathbf{r}_n \quad (3) $$

where

$$ {}^0\mathbf{T}_n(\mathbf{q}) = \prod_{i=1}^{n} {}^{i-1}\mathbf{T}_i = {}^0\mathbf{T}_1(q_1)\,{}^1\mathbf{T}_2(q_2)\cdots{}^{n-1}\mathbf{T}_n(q_n) \quad (4) $$

55-DOF WHOLE-BODY MODEL

A spatial digital human skeletal model with 55 DOF, as shown in Figure 1, is considered in this work. The model consists of six physical branches and one virtual branch. The physical branches include the right leg, the left leg, the spine, the right arm, the left arm, and the head. In these branches, the right leg, the left leg, and the spine start from the pelvis, while the right arm, left arm, and head start from the ending joint of the spine (z_{30}, z_{31}, z_{32}). The virtual branch contains six global DOFs, including three global translations (z_1, z_2, z_3) and three global rotations (z_4, z_5, z_6) located at the pelvis, and move the model from the origin (o-xyz) to the current pelvic position (z_4, z_5, z_6).

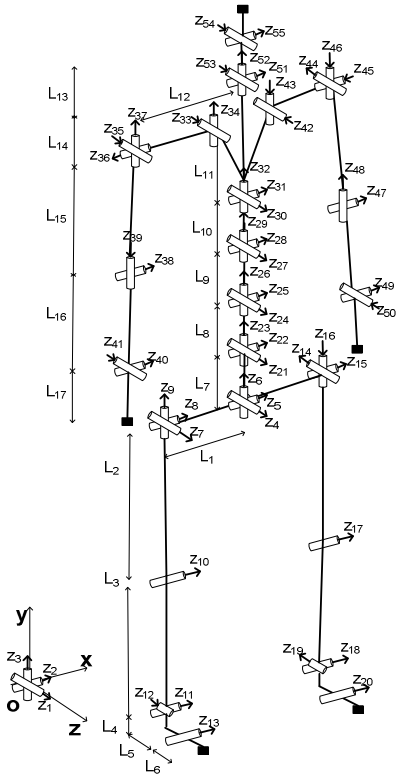

Figure 1. The 55-DOF digital human model

DYNAMICS MODEL

FORWARD RECURSIVE KINEMATICS

In this process, 4×4 transformation matrices $\mathbf{A}_j$, $\mathbf{B}_j$, and $\mathbf{C}_j$ are defined to represent the recursive position, velocity, and acceleration for the j^{th} joint respectively. Given the link transformation matrix ($\mathbf{T}_j$) and the kinematics state variables for each joint (q_j, $\dot{q}_j$, and $\ddot{q}_j$), then for j =1 to n we have:

$$\mathbf{A}_j = \mathbf{T}_1\ \mathbf{T}_2\ \mathbf{T}_3 \cdots \mathbf{T}_j = \mathbf{A}_{j-1}\mathbf{T}_j \tag{5}$$

$$\mathbf{B}_j = \dot{\mathbf{A}}_j = \mathbf{B}_{j-1}\mathbf{T}_j + \mathbf{A}_{j-1}\frac{\partial \mathbf{T}_j}{\partial q_j}\dot{q}_j \tag{6}$$

$$\begin{aligned}\mathbf{C}_j = \dot{\mathbf{B}}_j = \ddot{\mathbf{A}}_j = \mathbf{C}_{j-1}\mathbf{T}_j + 2\mathbf{B}_{j-1}\frac{\partial \mathbf{T}_j}{\partial q_j}\dot{q}_j \\ + \mathbf{A}_{j-1}\frac{\partial^2 \mathbf{T}_j}{\partial q_j^{\,2}}\dot{q}_j^{\,2} + \mathbf{A}_{j-1}\frac{\partial \mathbf{T}_j}{\partial q_j}\ddot{q}_j\end{aligned} \tag{7}$$

$\mathbf{A}_0 = [\ \mathbf{I}\ ]$ and $\mathbf{B}_0 = \mathbf{C}_0 = [\ \mathbf{0}\ ]$.

After obtaining all transformation matrices $\mathbf{A}_j$, $\mathbf{B}_j$, and $\mathbf{C}_j$, the global position, velocity, and acceleration of a point in the Cartesian coordinate system can be calculated using the following formulas:

$$^0\mathbf{r}_n = \mathbf{A}_n\mathbf{r}_n\,; \qquad ^0\dot{\mathbf{r}}_n = \mathbf{B}_n\mathbf{r}_n\,; \qquad ^0\ddot{\mathbf{r}}_n = \mathbf{C}_n\mathbf{r}_n \tag{8}$$

where $\mathbf{r}_n$ represents the augmented local coordinates of the point in the n^{th} coordinate system.

BACKWARD RECURSIVE DYNAMICS

Based on forward recursive kinematics, the backward recursion for the dynamic analysis is accomplished by defining a 4×4 transformation matrix $\mathbf{D}_i$ and 4×1 transformation matrices $\mathbf{E}_i$, $\mathbf{F}_i$, and $\mathbf{G}_i$, as follows.

Given the mass and inertia properties of each link, the external force $\mathbf{f}_k^{\mathrm{T}} = \begin{bmatrix} f_x & f_y & f_z & 0 \end{bmatrix}$, and the moment $\mathbf{h}_k^{\mathrm{T}} = \begin{bmatrix} h_x & h_y & h_z & 0 \end{bmatrix}$ for link k ($1 \le k \le n$) defined in the global coordinate system, the joint actuation torques τ_i for $i = n$ to 1 are computed as follows (Toogood, 1989):

$$\tau_i = tr\left[\frac{\partial \mathbf{A}_i}{\partial q_i}\mathbf{D}_i\right] + \mathbf{g}^{\mathrm{T}}\frac{\partial \mathbf{A}_i}{\partial q_i}\mathbf{E}_i + \mathbf{f}_k^{\ \mathrm{T}}\frac{\partial \mathbf{A}_i}{\partial q_i}\mathbf{F}_i + \mathbf{G}_i^{\mathrm{T}}\mathbf{A}_{i-1}\mathbf{z}_0 \tag{9}$$

$$\mathbf{D}_i = \mathbf{J}_i\mathbf{C}_i^{\mathrm{T}} + \mathbf{T}_{i+1}\mathbf{D}_{i+1} \tag{10}$$

$$\mathbf{E}_i = m_i\,^i\mathbf{r}_i + \mathbf{T}_{i+1}\mathbf{E}_{i+1} \tag{11}$$

$$\mathbf{F}_i = {}^k\mathbf{r}_f\,\delta_{ik} + \mathbf{T}_{i+1}\mathbf{F}_{i+1} \tag{12}$$

$$\mathbf{G}_i = \mathbf{h}_k\delta_{ik} + \mathbf{G}_{i+1} \tag{13}$$

where $\mathbf{D}_{n+1} = \mathbf{E}_{n+1} = \mathbf{F}_{n+1} = \mathbf{G}_{n+1} = [\ \mathbf{0}\ ]$; $\mathbf{J}_i$ is the inertia matrix for link i; m_i is the mass of link i; $\mathbf{g}$ is the gravity vector; $^i\mathbf{r}_i$ is the location of center of mass of link i in the local frame i; $^k\mathbf{r}_f$ is the position of the external force in the local frame k; $\mathbf{z}_0 = \begin{bmatrix} 0 & 0 & 1 & 0 \end{bmatrix}^{\mathrm{T}}$, and δ_{ik} is Kronecker delta.

The first term in the torque expression is the inertia and Coriolis torque, the second term is the torque due to gravity, the third term is the torque due to external force, and the fourth term represents the torque due to the external moment.

SENSITIVITY ANALYSIS

The gradients of the torque for the 3D human mechanical system with respect to the state variables $\frac{\partial \tau_i}{\partial q_k}$, $\frac{\partial \tau_i}{\partial \dot{q}_k}$, $\frac{\partial \tau_i}{\partial \ddot{q}_k}$ (i = 1 to n; k = 1 to n) can be evaluated in a recursive way using the foregoing recursive Lagrangian dynamics formulation (Equations (5)-(13)).

$$\frac{\partial \tau_i}{\partial q_k} = \begin{cases} tr\left(\frac{\partial^2 \mathbf{A}_i}{\partial q_i \partial q_k}\mathbf{D}_i + \frac{\partial \mathbf{A}_i}{\partial q_i}\frac{\partial \mathbf{D}_i}{\partial q_k}\right) + \mathbf{g}^{\mathrm{T}}\frac{\partial^2 \mathbf{A}_i}{\partial q_i \partial q_k}\mathbf{E}_i & (k \le i) \\ +\mathbf{f}^{\mathrm{T}}\frac{\partial^2 \mathbf{A}_i}{\partial q_i \partial q_k}\mathbf{F}_i + \mathbf{G}_i^{\mathrm{T}}\frac{\partial \mathbf{A}_{i-1}}{\partial q_k}\mathbf{z}_0 & \\ tr\left(\frac{\partial \mathbf{A}_i}{\partial q_i}\frac{\partial \mathbf{D}_i}{\partial q_k}\right) + \mathbf{g}^{\mathrm{T}}\frac{\partial \mathbf{A}_i}{\partial q_i}\frac{\partial \mathbf{E}_i}{\partial q_k} & (k > i) \\ +\mathbf{f}^{\mathrm{T}}\frac{\partial \mathbf{A}_i}{\partial q_i}\frac{\partial \mathbf{F}_i}{\partial q_k} & \end{cases} \quad (14)$$

$$\frac{\partial \tau_i}{\partial \dot{q}_k} = tr\left(\frac{\partial \mathbf{A}_i}{\partial q_i}\frac{\partial \mathbf{D}_i}{\partial \dot{q}_k}\right) \quad (15)$$

$$\frac{\partial \tau_i}{\partial \ddot{q}_k} = tr\left(\frac{\partial \mathbf{A}_i}{\partial q_i}\frac{\partial \mathbf{D}_i}{\partial \ddot{q}_k}\right) \quad (16)$$

GAIT MODEL

SYMMETRIC NORMAL GAIT

In the current work, normal walking is assumed to be symmetric and cyclic. As defined in the literature, a complete gait cycle includes two continuous steps (one stride). The step is further divided into two phases, the single support phase and the double support phase.

Considering the foot flexion, the two support phases can be detailed into four basic supporting modes: right foot single support (RSS), left foot single support (LSS), right foot leading double support (RDS) and left foot leading double support (LDS), as shown in Figure 2. In this work, the gait cycle starts from the left heel strike (LDS) and goes through the right swing (LSS), the right heel strike (RDS), and the right swing (RSS) before coming back to left heel strike (LDS) again. By applying the symmetry conditions, it is possible to consider only one step in a normal steady gait cycle instead of considering two steps. As a result, the computational costs are significantly minimized, as depicted in Figure 3.

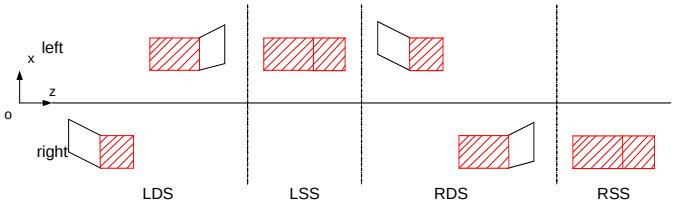

Figure 2. Four basic supporting modes (top view)

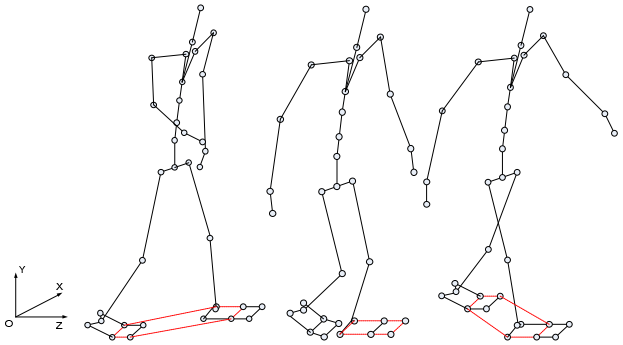

Figure 3. A normal step with initial and final postures

symmetry

GROUND REACTION FORCES

In the single support phase, one foot supports the whole body and the ZMP stays in the foot area so that ground reaction forces (GRF) can be applied at the ZMP directly. However, in the double support phase, the ZMP is located between the two supporting feet, and therefore, the resultant GRF needs to be distributed into the two feet appropriately. This distribution process can be treated as a sub-optimization problem (Dasgupta and Nakamura, 1999). In order to simplify this process, a linear relationship is used to distribute GRF in the double support phase as shown in Figure 4 (a).

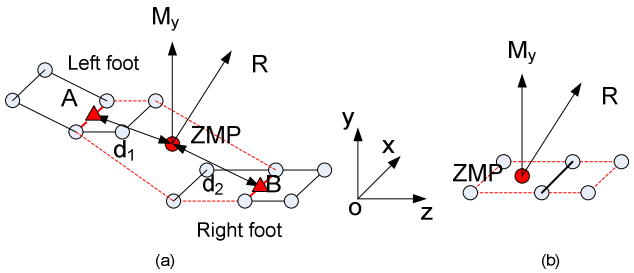

Figure 4. Applying ground reaction forces on ZMP

(a) double support phase, (b) single support phase

In Figure 4, points A and B (triangles) are center points of the middle joints of the feet. d_1 and d_2 are the distances from the ZMP (circles) to points A and B, respectively. Note that there are only normal moment M_y and resultant force $\mathbf{R}$ (R_x, R_y, R_z) at ZMP, as M_z and M_x vanish due to the assumption of no-slip condition. The GRF is linearly decomposed to the central points as follows:

$$M_{y1} = \frac{d_2}{d_1 + d_2} M_y; \quad \mathbf{R}_1 = \frac{d_2}{d_1 + d_2}\mathbf{R}$$

$$M_{y2} = \frac{d_1}{d_1 + d_2} M_y; \quad \mathbf{R}_2 = \frac{d_1}{d_1 + d_2}\mathbf{R} \quad (17)$$

In this work, a two-step algorithm is used to calculate GRF as depicted in the following flowchart.

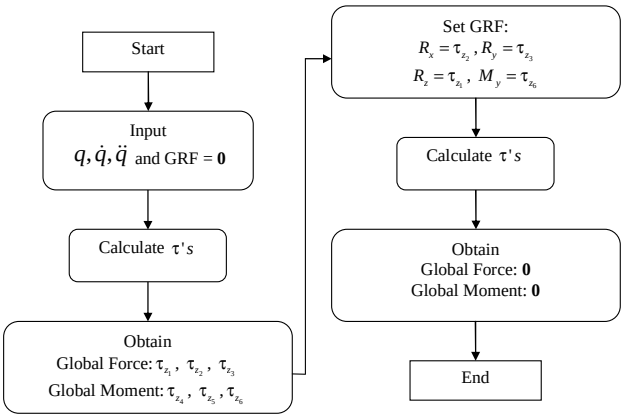

Figure 5. Flowchart of two-step algorithm to calculate GRF (a) without GRF, and (b) with GRF

First, given current state variables, the recursive Lagrangian dynamics of the whole body is used to calculate torques without GRF. The resulting global forces in the virtual branch are not zero because of excluding GRF; however, the moments about the *x* and *z* at ZMP are zero due to the ZMP calculation.

Second, GRF are assumed to be acting at the ZMP. Considering the equilibrium of the global forces and moments in the virtual branch with the ground reaction forces and moments, three forces and moment about the *y* axis at the ZMP are calculated. The GRF are then treated as external forces and moments for the entire model and the updated joint torques are recovered from the equations of motion.

OPTIMIZATION FORMULATION

DESIGN VARIABLES

In the current formulation, the design variables are the joint profiles $q_i(t)$ for a symmetric and cyclic gait motion. Besides the joint profiles, the initial posture is also optimized rather than specified from the experiment. Also, the final posture should satisfy the symmetry condition with the initial posture so that continuous joint profiles are generated. Meanwhile, the torque profiles are calculated from joint profiles using the recursive Lagrangian dynamics equations.

OBJECTIVE FUNCTION

The energy-related performance measure, the integral of the squares of all joint torques, is used as the objective function for the walking motion prediction that is defined as:

$$Minimize \quad f(\mathbf{q}) = \int_{t=0}^{T} \sum_{i=1}^{ndof} \tau_i^2(\mathbf{q}) dt \qquad (18)$$

where *ndof* is the number of degrees of freedom.

CONSTRAINTS

Several constraints are proposed and implemented in this work to satisfy laws of physics and boundary conditions through out the normal walking process. These constraints include Joint angle limits, ground penetration, foot contacting positions, ZMP stability, Pelvic velocity, soft impact, Knee flexion at mid-swing, symmetry conditions, and the arm-leg coupling.

Joint Angle Limits

The joint angle limits accounting for the physical range of motion are obtained from experiments:

$$\mathbf{q}^L \le \mathbf{q}(t) \le \mathbf{q}^U, \qquad 0 \le t \le T \qquad (19)$$

where $\mathbf{q}^L$ is the lower limit on the joint angles and $\mathbf{q}^U$ is the upper limit on the joint angles.

Ground Penetration

Bipedal walking is characterized with unilateral contact in the whole process. While the foot is in contact with the ground, the height of the contacting points is zero. The other points should be above the ground and the height greater than zero (Figure 6), as follows:

$$\begin{aligned} y_i(t) &= 0, \qquad 0 \le t \le T, \qquad i \in contact \\ y_i(t) &> 0, \qquad 0 \le t \le T, \qquad i \notin contact \end{aligned} \qquad (20)$$

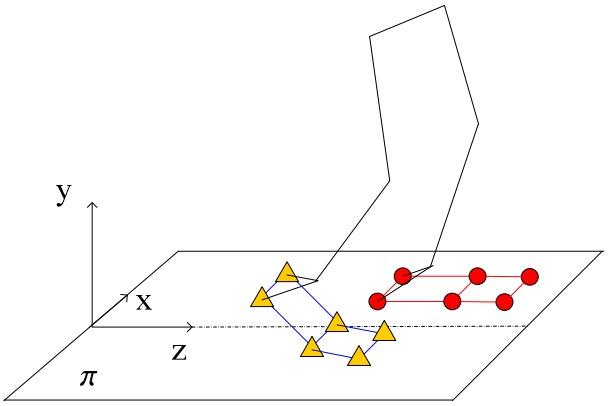

Figure 6. Foot ground penetration (circle: on the ground; triangle: above the ground)

Contacting Position

Since the step length *L* is given, the foot contacting position is known and specified at each time.

$$\mathbf{x}_i(t) = \tilde{\mathbf{x}}_i, \qquad i \in contact \qquad (21)$$

where $\tilde{\mathbf{x}}_i$ is the specified contacting position.

ZMP Stability

The stability is achieved by constraining the ZMP to be in the foot supporting region (FSR) (Vukobratović and Borovac, 2004).

$$z_{ZMP}(t) \in FSR, \qquad x_{ZMP}(t) \in FSR \qquad 0 \le t \le T \tag{22}$$

Pelvic Velocity

The pelvic translational velocity along the walking direction in normal walking is stable and almost a constant (*V*) quantity; this is treated as a constraint.

$$\dot{z}_{pelvis}(t) = V \qquad 0 \le t \le T \tag{23}$$

Soft Impact

The landing impact issue is taken into account by imposing velocity of contacting points to be zero. This is the so-called soft impact, which makes the gait motion gentle and smooth.

$$\begin{aligned} &\dot{x}_i(t) = 0, \quad \dot{y}_i(t) = 0, \quad \dot{z}_i(t) = 0, \\ &0 \le t \le T, \qquad i \in contact \end{aligned} \tag{24}$$

Knee Flexion at Mid-swing

Knee flexion at mid-swing is one of the six determinants of normal gait (Ayyappa, 1997). Biomechanical experiments show that the maximum knee flexion of normal gait is around 60 degrees regardless of age and gender. In addition, this also ensures enough space between the foot and the ground to avoid collision. This constraint is imposed as

$$q_{knee}(t) = 60 + \varepsilon, \qquad t = t_{midswing} \tag{25}$$

where ε is a small range of motion.

Symmetry Condition

The gait simulation starts from the left heel strike and ends with the right heel strike. The initial and final postures should satisfy the symmetry conditions. These conditions are expressed as

$$\begin{aligned} &q_{i\_left}(0) = q_{i\_right}(T) \\ &q_{jx}(0) = q_{jx}(T), \\ &q_{jy}(0) = -q_{jy}(T), \\ &q_{jz}(0) = -q_{jz}(T), \end{aligned} \tag{26}$$

where *x*, *y*, *z* are the global axes, and the subscript *i* represents the DOF of the leg, arm and shoulder joints and *j* represents other DOF.

Arm-Leg Coupling

The arm-leg coupling motion guarantees that the swing of the arm and leg on the same side are in the opposite directions.

$$\begin{aligned} &q_{right\_arm}(t) q_{right\_leg}(t) \le 0, \\ &q_{left\_arm}(t) q_{left\_leg}(t) \le 0, \qquad 0 \le t \le T \end{aligned} \tag{27}$$

NUMERICAL DISCRETIZATION

For the optimization problem, the entire time domain is discretized by B-spline curves, which are defined by a set of control points **P** and time grid points (knots) **t**. A B-spline is a numerical interpolation method that has many important properties, such as continuity, differentiability, and local control. These properties, especially differentiability and local control, make B-splines competent to represent joint angle trajectories, which require smoothness and flexibility.

Let $\mathbf{t} = \{ t_0, t_1, .., t_m \}$ be a non-decreasing sequence of real numbers, i.e., $t_i \le t_{i+1}, \ i = 0,.. ,m-1$. The t_i are called knots, and they are non-decreasingly spaced for a B-spline. A cubic B-spline is defined as

$$q(t) = \sum_{j=0}^{nct} N_{j,4}(t) P_j; \qquad 0 \le t \le T \tag{28}$$

where the $\{P_j\}$, $j = 0,..,nct$ are the $(nct+1)$ control points, and the $\{N_{j,4}(t)\}$ are the cubic B-spline basis functions defined on the non-decreasing knot vector.

Since the first- and second-order derivatives of the joint angles are needed in the optimization problem, the derivatives of a cubic B-spine curve can be easily obtained because only the basis functions are functions of time. Therefore, the original continuous variable optimization problem is transformed into a parameterized optimization problem by using Equations (28) and the following two equations:

$$\dot{q}(t) = \sum_{j=0}^{nct} \dot{N}_{j,4}(t) P_j; \qquad 0 \le t \le T \tag{29}$$

$$\ddot{q}(t) = \sum_{j=0}^{nct} \ddot{N}_{j,4}(t) P_j; \qquad 0 \le t \le T \tag{30}$$

q, $\dot{q}$, and $\ddot{q}$ are functions of **t** and **P**; therefore, torque $\tau = \tau(\mathbf{t}, \mathbf{P})$ is an explicit function of the knot vector and control points from the equation of motion. Thus, the derivatives of a torque τ with respect to the control points is computed using the chain rule as

$$\frac{\partial \tau}{\partial P_i} = \frac{\partial \tau}{\partial q}\frac{\partial q}{\partial P_i} + \frac{\partial \tau}{\partial \dot{q}}\frac{\partial \dot{q}}{\partial P_i} + \frac{\partial \tau}{\partial \ddot{q}}\frac{\partial \ddot{q}}{\partial P_i} \tag{31}$$

Finally, five control points are used for each DOF and thus we have 5×55 = 275 design variables and 629 nonlinear constraints.

NUMERICAL RESULTS

A large-scale sequential quadratic programming (SQP) approach in SNOPT (Gill et al., 2002) is used to solve the nonlinear optimization problem of normal walking. To use the algorithm, cost and constraint functions and their gradients need to be calculated. The foregoing developed recursive kinematics and dynamics formulations provide accurate gradients to improve the computational efficiency of the numerical optimization algorithm. The appropriate normal walking parameters (velocity and step length) are obtained from biomechanics literature (Inman et al., 1981). In addition to normal walking, the current work also considered situations where people walk and carry backpacks with various weights (0 lbs, 20 lbs, and 40 lbs). Each case requires about 600 cpu-seconds on a Pentium(R) 4 3.46 GHz computer.

NORMAL GAIT MOTION

To solve a normal gait motion, the user inputs a pair of parameters, for example, normal walking velocity V = 1.2 m/s and step length L = 0.7 m. Figure 7 shows the resulting stick diagram of a 3D human walking on flat ground. As expected, correct bending of knee occurs to avoid collision, and the arms swing to balance the leg swing and GRF. The continuity condition is satisfied to generate a smooth walking motion while the initial posture is also optimized. It is important to note that the spine remains upright automatically to reduce energy expenditure in the walking motion. In addition, the ZMP trajectory is smooth and stays in the support region

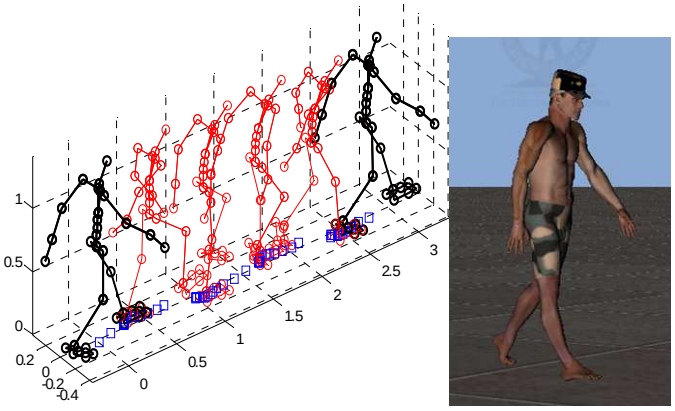

Figure 7. Stick diagram of optimized cyclic walking motion (square dot is ZMP)

Figure 8 depicts the torque profiles of the right hip, right knee, and right ankle. It is evident that the ankle torque is quite small in the swing phase and that the peak value occurs at the heel strike.

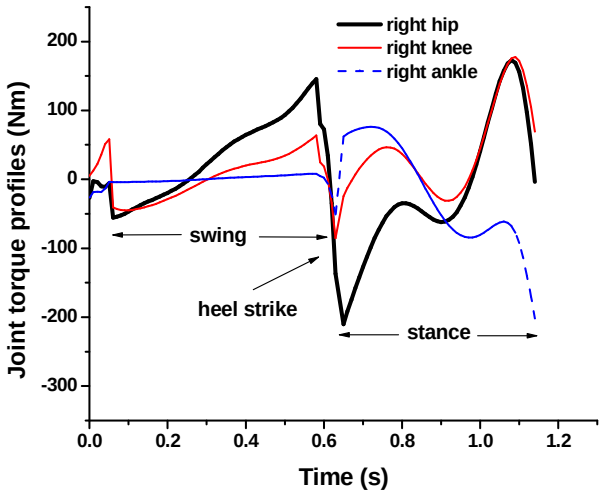

Figure 8. Joint torque profiles of right leg

NORMAL WALKING WITH BACKPACK

In this process, a shoulder backpack is considered in the walking motion prediction with the walking velocity V = 1.0 m/s and step length L = 0.5 m. Three cases are tried with varying backpack weights: 0 lbs, 20 lbs, and 40 lbs. 3D diagrams of the walking motion are compared in Figure 9, and reasonable spine bending is observed. The GRF are depicted as in Figure 10, and a heavier backpack results in larger GRF. The torque profile of the right knee is illustrated in Figure 11.

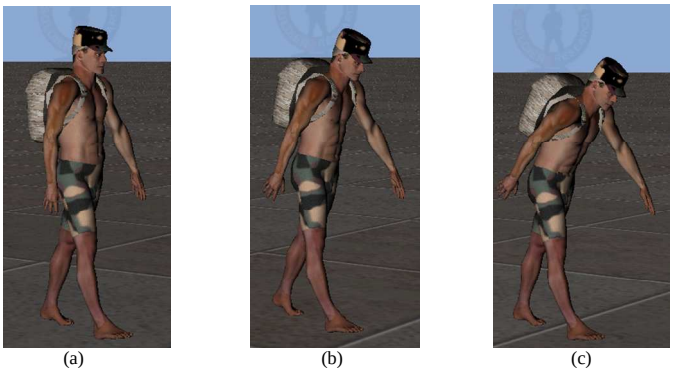

Figure 9. Normal walking with backpack: (a) 0 lbs; (b) 20 lbs; (c) 40 lbs

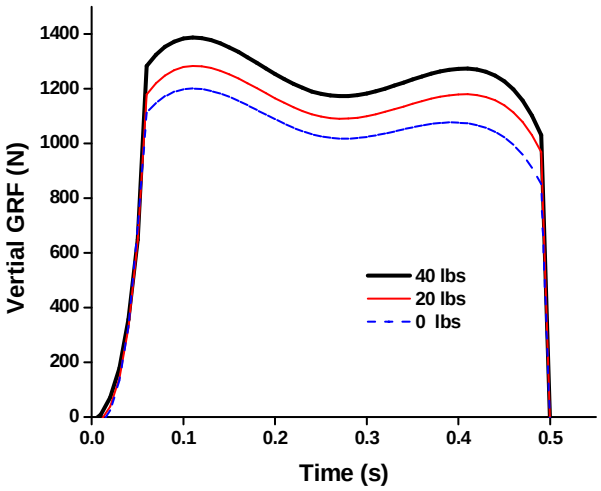

Figure 10. Vertical GRF of walking with backpack

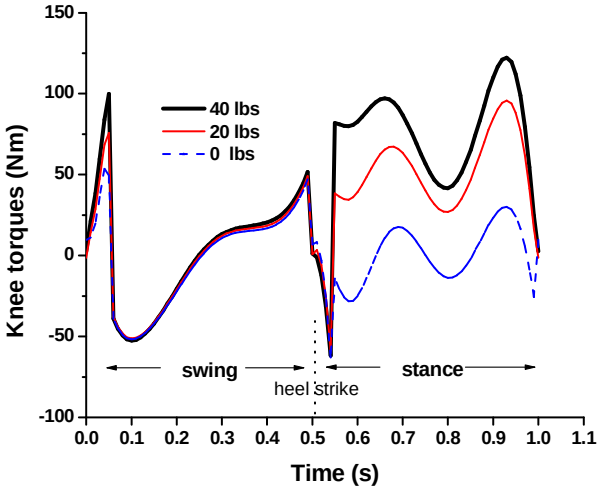

Figure 11. Torque profile of right knee with backpack

VALIDATION

In this work, two predicted walking determinants, the knee and ankle joint angle profiles, were chosen for comparison purposes with data obtained from four normal subjects as shown in Figure 12. These walking parameters are a subset of the six well-known walking determinants defined by Saunders et al. (1953).

The data predicted by the dynamic model for the knee and ankle joints were also added to Figure 12. The graphs clearly show that the predicted trend is in the range of normal in terms of joint angle amplitude and time history.

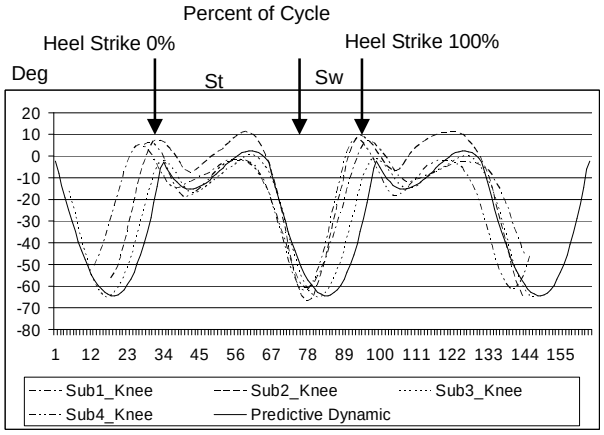

(a)

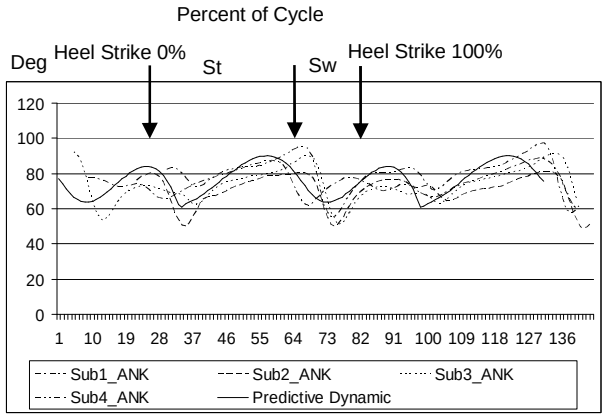

(b)

Figure 12. Verification of joint angle profiles of (a) knee and (b) ankle with experiments

CONCLUSION

In this paper, the motion prediction of the normal gait of a 55-DOF digital human model was presented. Based on the experimental data and biomechanical requirements, the results have demonstrated the ability of the proposed methodology to predict realistic human motions with the complex spatial skeleton model. The normal gait was treated as a cyclic and symmetric motion with repeatable initial and final postures. The motion planning was formulated as a large-scale nonlinear programming problem. Joint profiles were discretized using cubic B-splines, and the corresponding control points were treated as unknowns. The energy-related objective function, which represents the integral of squares of all joint torques, was minimized. The arm motion was incorporated by considering the role of the yawing moment and the arm-leg coupling motion constraints in the formulation. The walking determinants were obtained to verify the gait motion. The effect of backpack on gait motion was studied, and plausible posture responses were achieved. The kinetic data such as joint torque and ground reaction forces were also analyzed. The limitation of current gait formulation is that only energy-saved

motion is generated and the walking motion is on a level ground with symmetry conditions. Walking on uneven terrain and consideration of other performance measures such as maximizing speed, minimizing fatigue etc. are ongoing research topics.

ACKNOWLEDGMENTS

Support for this research provided by Natick's Biomechanical Simulator System (BAS), is gratefully acknowledged.

REFERENCES

1. Anderson, F.C. and Pandy, M.G. Dynamic optimization of human walking. Journal of Biomechanical Engineering, v 123(5), 2001, p 381-390.
2. Ayyappa, E. Normal human locomotion, part 1: basic concepts and terminology. Journal of Prosthetics and Orthotics, v 9(1), 1997, p 10-17.
3. Chevallereau, C. and Aousin, Y. Optimal reference trajectories for walking and running of a biped robot. Robotica, v 19, 2001, p 557-569.
4. Chung, H.J., Xiang Y., Mathai, A., Rahmatalla, S., Kim, J., Marler, T., Beck, S., Yang, J., Arora, J.S., Abdel-Malek, K. A robust formulation for prediction of human running. 2007 SAE Digital Human Modeling for Design and Engineering Conference, June 12-14, 2007, Seattle, Washington.
5. Dasgupta, A. and Nakamura, Y. Making feasible walking motion of humanoid robots from human motion capture data. IEEE international Conference on Robotics and Automation, v 2, May 1999, p 1044-1049.
6. Denavit, J. and Hartenberg, R.S. A kinematic notation for lower-pair mechanisms based on matrices. Journal of Applied Mechanics, v 77, 1955, p 215-221.
7. Gill, P.E., Murray, W., and Saunders, M.A. SNOPT: An SQP algorithm for large-scale constrained optimization. SIAM J. OPTIM. v 12, 2002, p 979-1006.
8. Huang, Q., Yokoi, K., Kajita, S., Kaneko, K., Arai, H., Koyachi, N. and Tanie, K. Planning walking patterns for a biped robot. IEEE Transactions on Robotics and Automation, 17, 2001, p 280-289.
9. Inman, V.T., Ralston, R.J. and Todd, F. Human walking. Baltimore, MD: Wilkins & Wilkins; 1981.
10. Kajita, S., Kanehiro, F., Kaneko, K., Fujiwara, K., Harada, K., Yokoi, K., and Hirukawa, H. Biped walking pattern generation by using preview control of zero-moment point. Proceedings of the IEEE International Conference on Robotics and Automation, 2003, Taipei, Taiwan, p 1620-1626.
11. Kim, H.J., Horn, E., Arora, J.S., and Abdel-Malek, K. An optimization-based methodology to predict digital human gait motion, 2005 Digital Human Modeling for Design and Engineering Conference, June 14 - 16, 2005, Iowa City.
12. McGuan, S. Human Modeling – From Bubblemen to Skeletons, 2001 SAE Digital Human Modeling for Design and Engineering Conference, June 26-28, 2001, Arlington, Virginia.
13. Mu, XP. and Wu, Q. Synthesis of a complete sagittal gait cycle for a five-link biped robot. Robotica, v 21, 2003, p 581-587.
14. Park, J. and Kim, K. Biped robot walking using gravity-compensated inverted pendulum mode and computed torque control. IEEE International Conference on Robotics and Automation, 4, 1998, p 3528-3533.
15. Saidouni, T. and Bessonnet, G. Generating globally optimized sagittal gait cycles of a biped robot. Robotica, v 21(2), 2003, p 199-210.
16. Sardain, P. and Bessonnet, G. Forces acting on a biped robot. Center of pressure - zero moment point. IEEE Transactions on Systems, Man and Cybernetics- Part A: Systems and Humans, v 34(5), 2004, p 630-637.
17. Saunders J.B., Inman V.T., and Eberhart H.D. The major determinants in normal and pathological gait. JBJS, 35-A, 1953, p 543-58.
18. Thelen, D.G., Anderson, F.C. and Delp, S.L. Generating dynamic simulations of movement using computed muscle control. Journal of Biomechanics. v 36, 2003, p 321-328.
19. Toogood, R.W. Efficient robot inverse and direct dynamics algorithms using micro-computer based symbolic generation. Proceedings of IEEE International Conference on Robotics and Automation, v 3, 1989, p 1827-1832.
20. Vukobratović, M. and Borovac, B. Zero-moment point – thirty five years of its life. International Journal of Humanoid Robotics, v 1(1), 2004, p. 157-173.
21. Yamaguchi, J., Soga, E., Inoue, S. and Takanishi, A. Development of a bipedal humanoid robot control method of whole body cooperative dynamic biped walking. IEEE International Conference on Robotics and Automation, v 1, 1999, p 368-374.

CONTACT

Corresponding author: J.S. Arora. Email: jasbir-arora@uiowa.edu; telephone: (319) 335-5658; fax: (319) 335-5660.